

Thermal Chemistry of 1,4-Difluoro-2-butenes on Pt(111) Single-Crystal Surfaces

Ilkeun Lee, Michael K. Nguyen, Thomas H. Morton, and Francisco Zaera*

Department of Chemistry, University of California, Riverside, California 92521

Received: May 16, 2008; Revised Manuscript Received: July 2, 2008

The thermal chemistry of *cis*- and *trans*-1,4-difluoro-2-butenes on Pt(111) single-crystal surfaces was characterized by temperature programmed desorption (TPD) and reflection–absorption infrared spectroscopy (RAIRS). The study was motivated by the possibility of differentiating the two isomers directly by mass spectrometry, something that is not possible with the nonfluorinated olefins. On the clean surface a preference was identified for the conversion of the *cis* isomer to its *trans* counterpart, the opposite to what had been previously reported with regular 2-butenes on hydrogen (or deuterium)-predosed Pt(111). Indeed, the formation of *trans*-1,4-difluoro-2-butene from the adsorbed *cis* isomer occurs at around 260 K, as identified directly by RAIRS and in the gas phase by mass spectrometry. Some *cis* is also formed from the *trans*, but only in a small yield and at much higher temperatures (~315 K). The preference for *trans*-to-*cis* conversion with the nonfluorinated olefins may therefore be explained by a reversal in adsorption stability induced by coadsorbed hydrogen. It was also determined that significantly more hydrogenation of the fluorinated olefins to their fluorinated alkanes occurs upon coadsorption with hydrogen or deuterium compared with what is seen with the regular olefins. Finally, the inductive effect of the fluorine substitutions leads to some changes in the high-temperature conversion of the adsorbed species.

1. Introduction

The thermal chemistry of olefins on single-crystal transition metal surfaces has been studied extensively by us^{1–4} and others,^{5–8} mainly in connection with their relevance to catalytic processes. However, some mechanistic details remain unresolved still. Specifically, the factors that determine selectivity in double-bond isomerization reactions, in both double-bond migration^{9,10} and *cis*–*trans* interconversion,^{11–14} are not fully known. Those reactions are believed to take place by following the so-called Horiuti–Polanyi mechanism,¹⁵ which involves the half-hydrogenation of the adsorbed olefin to an alkyl surface intermediate and the subsequent β -hydride elimination from that moiety back to another olefin. The hydrogenation–dehydrogenation steps have been well established, but not characterized in sufficient detail to fully explain the overall isomerization reactions: additional consideration must be given to the preferential removal of a particular H atom from the alkyl intermediate if that species possesses more than one regio- or stereodifferent hydrogen atom at the β positions.^{16,17}

Given that the mass spectra of the *cis* and *trans* isomers of most olefins are quite similar, it is difficult to study their interconversion directly with a surface-science approach, at least one based on temperature-programmed desorption (TPD). Instead, we have recently used H–D exchange as a proxy for that isomerization process, by taking advantage of the fact that each deuterium atom incorporation into the olefin is accompanied by a switch from one isomer to the other.¹¹ It was determined that, in the case of 2-butenes adsorbed on hydrogen (or deuterium)-predosed Pt(111) surfaces, *trans*-to-*cis* isomerization is preferred over the reverse *cis*-to-*trans* rearrangement, a conclusion that was also corroborated directly by infrared spectroscopy. This observation is justified at least in part by the observed higher stability of the adsorbed *cis* butene, but also suggests an easier β -hydride elimination from the 2-butyl

surface intermediate to form *cis* rather than *trans* olefins. Surprisingly, the opposite was recently seen on clean Pt(111).¹⁴ In search of an explanation for this discrepancy, and based on preliminary quantum mechanical calculation indicating a change in the relative energetics of this system upon hydrogen (or deuterium) addition to the surface,¹⁸ additional research was designed based on the use of 1,4-difluoro-2-butenes. The rationale behind this choice of reactants was the expectation that the *cis* and *trans* difluoro-labeled olefins may display different mass spectra, and therefore allow for the *cis*–*trans* TPD isomerization experiments to be carried out on the clean Pt(111) surface, without the need of coadsorbed deuterium.

Here we report on the key results that derived from those studies. It was found that, indeed, the two isomers of 1,4-difluoro-2-butene do display sufficiently different mass spectra to distinguish them in TPD experiments. It was then determined that the isomerization of *cis* butene to its *trans* counterpart is preferred over the reverse reaction on the clean Pt(111). This is opposite to what had been seen with the regular olefins on hydrogen-predosed surfaces. In addition, it was observed that the inductive effect of the fluorine substitutions leads to a change in selectivity when in the presence of coadsorbed hydrogen (or deuterium) toward hydrogenation to difluorobutane instead of molecular desorption of the isomerized olefins. Such a significant inhibition of β -hydride elimination steps from surface moieties, which has already been identified in other systems,^{19–21} hindered the study of the *cis*–*trans* isomerization reaction in the presence of coadsorbed hydrogen in this case, but provided additional insight on the chemistry of the adsorbed olefins. Other changes were observed in the high-temperature decomposition of the surface species as compared to those reported previously for 2-butenes.

2. Experimental Section

All temperature-programmed desorption (TPD) and reflection–absorption infrared spectroscopy (RAIRS) experiments

* Corresponding author. E-mail: zaera@ucr.edu.

were performed in a two-level ultrahigh vacuum (UHV) chamber cryopumped to a base pressure of less than 3×10^{-10} Torr.^{22,23} The main stage of this chamber is used to carry out the sample cleaning and TPD experiments, which are performed by means of a UTI 100C quadrupole mass spectrometer retrofitted with a retractable nose cone terminated in a 5-mm-diameter aperture. That aperture can be placed within 1 mm of the single crystal for the selective detection of molecules desorbing from the front surface of the crystal. The mass spectrometer is interfaced to a personal computer capable of monitoring the time evolution of up to 15 different masses in a single TPD experiment. A constant heating rate of 10 K/s was used in all TPD runs by using homemade electronics, and a bias of -100 V was applied to the crystal to avoid any chemistry induced by stray electrons from the ionizer of the ion gauge or the mass spectrometer.²⁴

The second level of our chamber, accessible by using a long-travel manipulator, is dedicated to the RAIRS experiments. The IR beam from a Bruker Equinox 55 FT-IR spectrometer is passed through a polarizer and focused through a NaCl window onto the sample at grazing incidence ($\sim 85^\circ$). The reflected beam then travels through a second NaCl window, and is focused onto a narrow-band mercury–cadmium–telluride (MCT) detector. The entire beam path is enclosed in a sealed box purged with dry air, purified by using a scrubber (Balston 75-60) for CO_2 and water removal. All spectra were taken at a surface temperature of ~ 80 K by averaging the data from 2000 scans acquired at a resolution of 4 cm^{-1} , a process that takes about 4 min per experiment, and ratioed against spectra from the clean sample obtained in the same way before gas dosing.

The Pt(111) single crystal, a disk 8 mm in diameter and 2 mm in thickness, was spotwelded to a pair of tantalum wires attached to the copper electrical feedthroughs of the sample manipulator. This arrangement allows for the crystal to be cooled to approximately 80 K by using a continuous flow of liquid nitrogen through the air side of the feedthroughs, and to be heated resistively to up to 1100 K. The temperature is measured with a chromel–alumel thermocouple spotwelded to the side of the crystal, and controlled by using the homemade feedback electronics mentioned above. The sample was routinely cleaned by cycles of oxidation in 2×10^{-6} Torr of oxygen at 700 K and annealing in vacuum at 1100 K, and occasionally by Ar^+ sputtering, although this latter procedure was minimized to minimize the creation of surface defects.

The *cis*- and *trans*-1,4-difluoro-2-butenes were synthesized from their corresponding commercially available *cis*- and *trans*-dichloro analogues (Acros, both 95% purity) via a procedure similar to what was previously described in the literature.²⁵ Either *cis*- or *trans*-1,4-dichloro-2-butene (5.0 g, 32.0 mmol) was heated with anhydrous potassium fluoride (6.0 g, 102.8 mmol) in anhydrous diethylene glycol at 400 K for 30 min while continuously distilling the corresponding volatile 1,4-difluoro-2-butene product out of the reaction mixture. The crude liquid was further distilled to give final yields of approximately 50% in both cases. The boiling points of both liquids were measured as 297 K at 250 Torr and 347 K at 760 Torr. ^1H NMR spectroscopy signatures (300 MHz, CCl_4): *cis* δ 4.92 (dm, $J_{\text{HF}} = 44$ Hz, 4 H), 5.95 (m, 2 H); *trans* δ 5.00 (dm, $J_{\text{HF}} = 45$ Hz, 4 H), 5.87 (m, 2 H). GC-mass spectra (70 eV) m/z (rel intensity): *cis* 41 (20), 46 (58), 59 (100), 72 (10), 77 (28), 92 (25); *trans* 41 (14), 46 (56), 59 (100), 72 (10), 77 (19), 92 (20). No impurities were detectable in the gas chromatographic trace in either case.

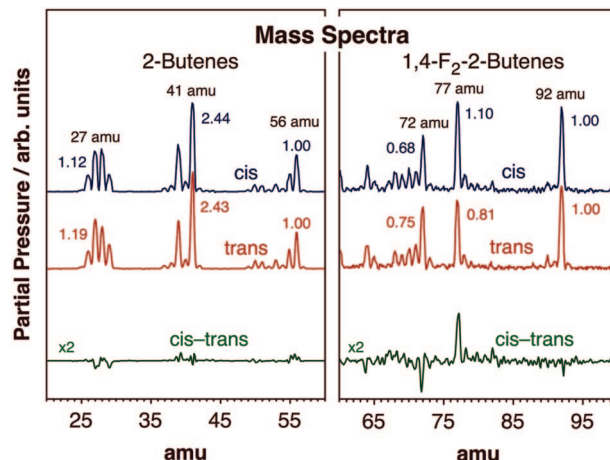


Figure 1. Mass spectra for normal (left) and 1,4-difluoro-substituted (right) *cis* and *trans* 2-butenes. The spectra for the two isomers of the regular butenes are virtually the same, so they cannot be differentiated in temperature-programmed desorption (TPD) experiments. The data for the difluoro compounds, on the other hand, show small but significant differences. The signals for m/z 72, 77, and 92 were used to determine the partition of the desorbing products between the *cis* and *trans* isomers.

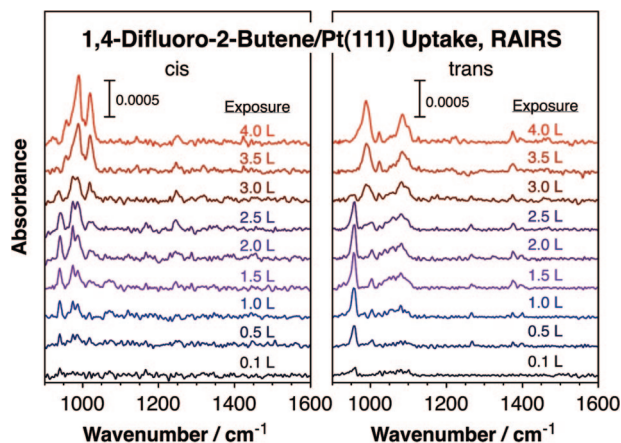


Figure 2. Reflection–absorption infrared spectra (RAIRS) as a function of initial exposure for *cis*- (left) and *trans*-1,4-difluoro-2-butenes (right) adsorbed on a Pt(111) single-crystal surface below 100 K. A vibrational assignment of the main features seen here is provided in Table 1. In general terms, a defined flat geometry and di- σ bonding are seen in both cases up to exposures of approximately 2.5 L, after which a collective conversion to a weaker π species is observed.

Reference mass spectra for the normal and difluoro-substituted 2-butenes were also obtained with our instrument to acquire the peak intensity information required for the deconvolution of the TPD data reported in Figures 3 and 4; they are shown in Figure 1. Notice that while the spectra of the two normal 2-butene isomers are virtually identical (Figure 1, left panel), those of the difluoro compounds show small but significant differences (right panel). Those differences are highlighted in the bottom trace, which was obtained by subtracting the trace for the *trans* isomer from that of the *cis*. It is clear that the *cis* compound yields a larger peak for m/z 77 and a smaller peak for m/z 72, in relative terms, than the *trans* counterpart. The differences seen with the in situ quadrupole mass spectrometer are somewhat smaller than those measured with the GC/MS instrument but show the same trends, due mainly to the differences in relative abundance of methyl radical loss (m/z 77) and HF expulsion (m/z 72) from the molecular ions. The fragmentation pathways and the differences between isomers

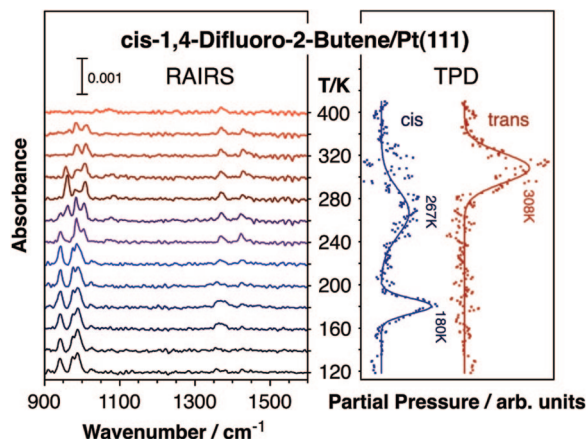


Figure 3. RAIRS vs temperature (left) and difluorobutene TPD (right) data from a monolayer (2.5 L) of *cis*-1,4-difluoro-2-butene adsorbed on Pt(111). The TPD traces have been obtained by deconvolution of the raw data obtained for m/z 72, 77, and 92 by using a methodology described in detail elsewhere.³² Significant isomerization to the *trans* isomer is seen around 300 K by both TPD and RAIRS techniques.

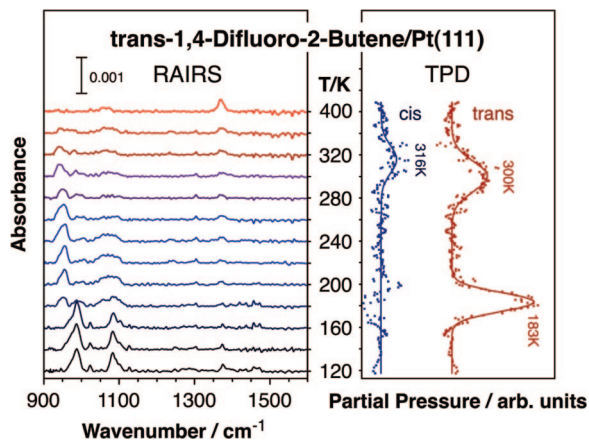


Figure 4. RAIRS vs temperature (left) and difluorobutene TPD (right) data from a monolayer (2.5 L) of *trans*-1,4-difluoro-2-butene adsorbed on Pt(111). Again, the TPD traces have been deconvoluted from the raw data as in Figure 3. Only minor isomerization to the *cis* isomer is seen, and at relatively high temperatures (around 320 K).

were confirmed by mass-analyzed ion kinetic energy spectroscopy (MIKES) of metastable ion decomposition of the m/z 92 parent ions, using liquid samples introduced into a reverse Nier-Johnson double-focusing mass spectrometer.

Hydrogen gas (>99.995% purity) was obtained from Liquid Carbonic, and deuterium (>99.5% atom purity), *cis*-2-butene (>95% purity), and *trans*-2-butene, (>95% purity) from Matheson. All gases were used as supplied, but their purities were frequently checked by mass spectrometry. The liquid samples were cleaned via a series of freeze–pump–thaw cycles before use, and their purities checked *in situ* by mass spectrometry. Exposures of the surface to the different chemicals were performed by backfilling of the vacuum chamber, and are reported in Langmuirs (1 Langmuir $\equiv 10^{-6}$ Torr·s), not corrected for differences in ion gauge sensitivities. Dosing was done at temperatures below 100 K unless otherwise indicated.

3. Results and Discussion

3.1. Low-Temperature Uptake. First, the uptake of both *cis*- and *trans*-1,4-difluoro-2-butenes following adsorption on the Pt(111) single-crystal surface at liquid nitrogen temperatures was characterized by RAIRS. The resulting spectra as a func-

tion of exposure for both isomers are shown in Figure 2, and the peak assignment for the main features seen in those data provided in Table 1. The assignments have been made by comparison with the IR spectra of the pure liquid samples, and also with the aid of reported assignments for nonfluorinated *cis*- and *trans*-2-butenes,¹⁴ 1-bromo-2-butene,²⁶ *trans*-1-fluoro-1-butene,²⁷ and 3,3,3-trifluoropropene.²⁸ The first thing to notice from the data in Figure 2 is that there is a distinct transition in both cases at about 2.5 L, manifested not only by the appearance of new features in the spectra but also by the disappearance of some of the peaks seen at lower exposures. This suggests a collective rearrangement of all the molecules adsorbed directly on the surface, not just the deposition of a second type of species in the first layer or a condensation in multilayers. This is an unexpected result: the uptake of regular olefins,^{14,29} including the cases of propene³ and all regular butenes¹⁴ on Pt(111), typically display a transition from di- σ to π bonding on the surface, but in the form of a buildup of the second species on top of the first. We do not have at present a full explanation for this difference, but it may be the result of an overall weakening of the bonding of the olefin to the surface upon fluorine substitution.

In any event, the RAIRS data in Figure 2 are consistent with di- σ adsorption at low coverages and π bonding at monolayer saturation. They also reflect an adsorption geometry with the central carbon–carbon double bond parallel to the surface at all times. Di- σ bonding is mostly indicated by red shifts in the frequencies of several of the stretching and deformation modes of the molecule. For instance, in the case of the *cis* isomer, the main out-of-plane deformation of the central C–H bonds, $\delta_{oop}(=C-H)$, is seen at 975 and 987 cm^{-1} in the low coverage regime but at 990 cm^{-1} in the saturated layer. For the *trans* molecule the corresponding peaks are seen at 957 and 988 cm^{-1} , respectively, and those for the C–F bond stretching, $\nu(C-F)$, at 1003 (low coverage) and 1022 (saturation) cm^{-1} . The fact that the $\delta_{oop}(=C-H)$ peak is one of the most prominent in all the spectra also speaks to the issue of flat adsorption, since only the dynamic dipole component perpendicular to the surface contributes to the intensity of RAIRS spectra with transition metals.^{30,31} Signals are also seen in some instances for terminal C–C stretching, $\nu(C-C)$, and CH_2 scissoring, $\gamma(\text{CH}_2)$, and wagging, $\omega(\text{CH}_2)$, modes, but never for the stretching of the central C–C bond, $\nu(C=C)$: the latter is therefore likely to be aligned parallel to the surface.

3.2. Thermal Chemistry on Clean Pt(111). Next we discuss the data obtained for the thermal conversion of the adsorbed 1,4-difluoro-2-butenes on clean Pt(111) surfaces. Sets of RAIRS traces as a function of annealing temperature (left panels) and difluorobutene TPD results (right) are reported in Figures 3 and 4 for the *cis* and *trans* isomers, respectively. Shown are the TPD traces obtained after deconvolution of the raw data for m/z 72, 77, and 92 following a procedure described in detail elsewhere.³² A first transition is observed in the RAIRS data with both isomers at about 180 K, the temperature at which molecular desorption is seen in the TPD results. The change is more dramatic in the case of the *trans* isomer, where the new spectra are completely different in appearance from the ones seen before, but that is only a reflection of differences in the starting rather than the ending point of these experiments; the initial coverage of the *trans* isomer seems to be slightly higher than that of the *cis* in the data reported here. In both cases the spectra obtained above 180 K correspond to submonolayer coverages: notice their similarities with the corresponding results obtained for low temperatures and exposures below 2.5 L (Figure 2).

TABLE 1: Vibrational Assignment for the RAIRS Data of *cis*- and *trans*-1,4-Difluoro-2-butenes Adsorbed on Pt(111)^a

mode	<i>cis</i> -1,4-difluoro-2-butene				<i>trans</i> -1,4-difluoro-2-butene		
	80 K, 0–3 L	80 K, 4 L	280 K	320 K	80 K, 0–3 L	80 K, 4 L	300 K
$\nu(\text{C-F})_{\text{gauche}}$	942 (s)		941 (m)		945 (sh)		938 (m)
$\delta_{\text{oop}}(\text{=C-H})$	975 (s), 987 (s)	957 (m), 990 (vs)	962 (s), 985 (vs)	962 (w), 986 (s)	957 (s)	967 (sh), 988 (vs)	982 (w)
$\nu(\text{C-F})$	1018 (w)	1020 (vs)	1004 (s)	1010 (s)	1003 (w)	1022 (w)	1004 (vw)
$\rho(\text{CH}_2)$			1035 (vw)	1032 (vw)	1038 (w), 1061 (w)	1048 (w)	1060 (w)
$\nu(\text{C-C})$			1062 (w), 1078 (w)		1081 (m)	1082 (s), 1102 (m), 1126 (w)	1080 (w)
$\rho_s(\text{=C-H})$	1242 (vw)					1220 (w)	
$\tau(\text{CH}_2)$	1257 (w)	1250 (w)			1268 (vw)		
$\delta_{\text{ip}}(\text{=C-H})$					1304 (vw)		1303 (w)
$\omega(\text{CH}_2)$		1367 (vw)	1370 (m)	1370 (m)	1374 (m), 1400 (w)	1374 (m), 1397 (w)	1362 (m), 1378 (w)
$\gamma(\text{CH}_2)$	1435 (w)	1422 (w)	1423 (m), 1442 (w)	1427 (m), 1442 (w)		1455 (vw), 1468 (w)	
$\nu_s(\text{CH}_2)$						2900 (m, br)	2910 (w, br)
$\nu_a(\text{CH}_2)$			2915 (m)	2915 (m)	2982 (w)	2950 (m, br)	2945 (w, br)
$\nu(\text{=C-H})$			3013 (m)	3013 (m)	3060 (m)	3060 (w)	3018 (m)

^a All frequencies are reported in cm^{-1} . Modes: ν = stretching, δ = deformation, ρ = rocking, τ = twisting, ω = wagging, γ = scissoring. Subindices: oop = out of plane, ip = in plane, s = symmetric, a = asymmetric. Intensities: vs = very strong, s = strong, m = medium, w = weak, vw = very weak, sh = shoulder, br = broad.

The next transition in the case of the *cis* isomer is seen at about 240 K. In fact, molecular *cis*-1,4-difluoro-2-butene desorption starts already around 220 K (and peaks at 267 K) in the TPD experiments, even if that amounts to less than 40% of the total desorption from the monolayer. The RAIRS data in the 260–300 K range reflect the isomerization of the *cis* adsorbate to its *trans* isomer: new bands develop for the $\delta_{\text{oop}}(\text{=C-H})$, $\nu(\text{C-F})$, $\nu(\text{C-C})$, and $\nu(\text{=C-H})$ at 962, 1004, 1078, and 3013 cm^{-1} , respectively. Desorption of the *trans* isomer is then seen at about 308 K, accounting for the remaining >60% of the monolayer molecular olefin desorption. A similar transition is not evident in the data for the *trans* isomer, because no significant double bond isomerization occurs in that case. Some *cis*-1,4-difluoro-2-butene is detected in the TPD experiments, but only less than 20% of the total monolayer butene desorption, and in a peak at 316 K, a temperature ~ 15 K higher than that required for the desorption of the original *trans* molecule.

The results described in the previous paragraph indicate a preference for the isomerization of *cis*-1,4-difluoro-2-butene to its *trans* counterpart on the clean Pt(111) surface. That preference can be explained, at least in part, by the higher stability of the initial adsorbate in the monolayer: while the *cis* olefin desorbs at 267 K, the *trans* isomer does so at 300 K. Surprisingly, though, this trend is opposite to that seen with normal 2-butenes, for which a more stable *cis* adsorbate and a preferential *trans*-to-*cis* conversion have been reported.^{11,12} The difference appears to be related to the initial conditions of the surface used in the two sets of experiments. The conclusions for the normal (nonfluorine-substituted) 2-butenes are based on results from H–D exchange studies, since the isomerization reaction could not be followed directly by TPD (the spectra of the two isomers are nearly identical, Figure 1), and those required the coadsorption of deuterium on the surface. The data reported here, in contrast, correspond to experiments on clean Pt(111). It is well-known that hydrogen (or deuterium) coadsorption weakens the binding of olefins to metal surfaces (and favors π instead of di- σ interactions).^{2,8,33–36} In this case, recent density-functional theory (DFT) calculations in our group indicate that, in relative terms, hydrogen coadsorption reverses

the stability of the *cis* and *trans* isomers: while the di- σ *trans* species is the most stable on clean Pt(111), the π *cis* olefin displays a higher adsorption energy on the H-saturated surface.¹⁸ Therefore, the reversal in selectivity can be ascribed directly to an effect due to coadsorbed hydrogen.

One final point here: according to the Horiuti–Polanyi mechanism, *cis*–*trans* isomerization occurs via an initial half-hydrogenation step to form an alkyl intermediate, which requires the incorporation of surface hydrogen atoms. However, only a small amount of hydrogen is required for this, because those H atoms act as catalysts, and are released by the subsequent β -hydride elimination step back to the olefin. Small amounts of hydrogen are always present in these systems, originating from adsorption from the background or from dehydrogenation of some of the adsorbed olefin (see Figure 6). We do not believe that this affects the relative behavior between the *cis* and *trans* olefins, since they both display very similar H₂ TPD traces.

3.3. Thermal Chemistry on Hydrogen- and Deuterium-Predosed Pt(111). To test the influence of hydrogen coadsorption on the energetics and reactivity of the 1,4-difluoro-2-butenes, and also to explore the kinetics of hydrogenation and H–D exchange with those adsorbates, additional TPD experiments were carried out on hydrogen-precured Pt(111). Figure 5 reports representative data for the cases of 1.0 L of either *cis*- or *trans*-1,4-difluoro-2-butene adsorbed on surfaces predosed with 20 L of H₂ or D₂. Key traces are shown in this figure for the m/z 72–77 and 92–96 ranges, but data were also collected for the m/z 51–65 range (not shown) to corroborate our assignments.

In general terms, two sets of desorption peaks are observed in all the experiments, around 185–190 and 220–230 K, corresponding to molecular 1,4-difluoro-2-butene and 1,4-difluorobutane desorption, respectively. Molecular adsorption is probably weakened by the presence of the coadsorbed hydrogen, but that cannot be directly assessed because hydrogenation already occurs at low temperatures, at approximately 100 K below the temperatures required for olefin desorption from the clean surface (compare the data in Figures 3 and 4 with those in Figure 5). That hydrogenation temperature shifts gradually with coverage: while alkane desorption from surfaces

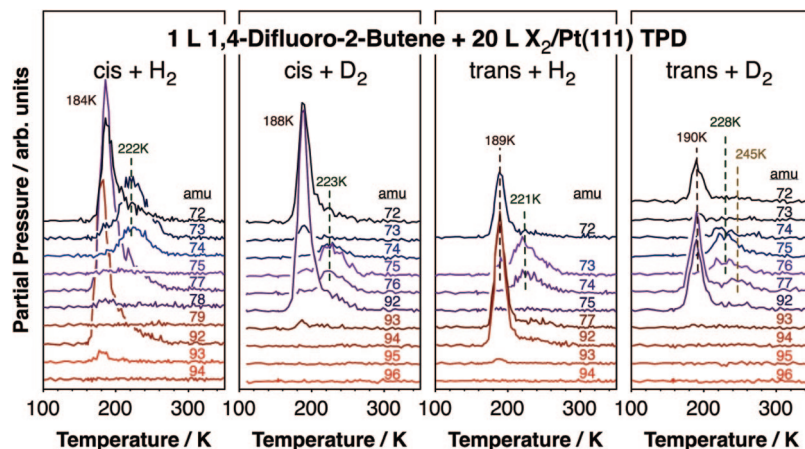


Figure 5. TPD for both *cis*- (two left panels) and *trans*- (right two) 1,4-difluoro-2-butenes adsorbed on Pt(111) predosed with either hydrogen (first panel of each set) or deuterium (second panels). Shown are the signals recorded for the relevant masses in the m/z 72 to 96 range. Molecular olefin desorption is seen in all cases at approximately 185–190 K, and 1,4-difluorobutane, normal and dideuterated for the H- and D-predosing cases respectively, is detected at around 220 K. Notice that a small amount of 1,4-difluorobutane- d_3 (m/z 77) is also seen in the last panel, at about 245 K, indicative of some H–D exchange within the adsorbed olefin prior to its full deuteration to the alkane.

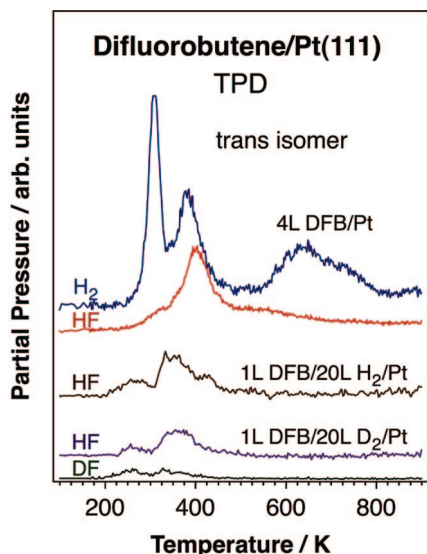


Figure 6. Hydrogen and hydrogen fluoride TPD from *trans*-1,4-difluoro-2-butene adsorbed on clean (top two traces) and hydrogen- (middle) and deuterium (two bottom traces)-predosed Pt(111) surfaces. On the clean substrate hydrogen desorption from dehydrogenation of the surface species occurs in three main stages, around 310, 385, and 640 K, while HF production is observed mostly about 400 K. Hydrogen coadsorption leads to a reduction in desorption temperature for HF, to approximately 270 and 350 K. With deuterium significant DF is also detected, pointing to extensive isotope exchange within the adsorbed olefin.

predosed with 20 L of hydrogen (or deuterium) peaks at around 220 K, in the case of 10 L of H_2 it peaks at around 200 K (data not shown). Similar shifts have been observed before with the normal 2-butenes, but the products there always desorb at higher temperatures than the difluoro-substituted molecules studied here.¹² Finally, higher desorption temperatures were seen with the *trans* difluorobutene isomer, as on the clean Pt(111), but the differences are small and may not be significant.

Appreciable hydrogenation is manifested by the peaks seen at ~ 225 K, as mentioned above. For the cases of normal hydrogen coadsorption, this is reflected mainly in the signals for m/z 73 and 74, since no measurable intensity can be seen for difluorobutane in the traces above m/z 92. In the experiments with D_2 , the equivalent chemistry is indicated by the peaks observed for m/z 75 and 76, which can be logically assigned to

1,4-difluoro-2,3-dideuterobutane. In addition, a feature is also detected for m/z 77 at about 245 K associated with a trideutero-substituted alkane, indicating a degree of H–D exchange on the surface species at these higher temperatures. The isotope exchange is in fact fairly extensive, as shown by the desorption of significant amounts of deuterium fluoride upon decomposition of the adsorbates at higher temperatures (see below), but only takes place in the high-temperature tail of the alkane desorption. This is more clearly seen in the data obtained for surfaces predosed with only 10 L of D_2 (data not shown), where two distinct alkane peaks are seen at about 220 and 240 K, and where the trideuterio molecules are observed mainly in the latter (data not shown). Even multiple H–D exchange is possible there: broad peaks due to 1,4-difluorobutane- d_4 are detected at ~ 265 and ~ 250 K for the *cis* and *trans* isomers, respectively, in the m/z 78 traces (data not shown). The yields for both hydrogenation and H–D exchange reactions are about 50% higher with the *trans* isomer, and all are much higher than with the normal butenes (for which almost no hydrogenation occurs).¹²

3.4. High-Temperature Chemistry. According to the RAI-RS data in Figures 3 and 4, another chemical transformation takes place on the surface with the *cis* isomer at approximately 300 K, after all molecular desorption is complete, and a final conversion occurs with both isomers above ~ 350 K. All the high-temperature RAI-RS are dominated by the CH_2 wagging, $\omega(CH_2)$, peak at 1370 cm^{-1} , so the terminal monofluoromethyl groups appear to survive the thermal treatment, and perhaps become oriented with their central axis close to parallel to the surface. In the case of the *cis* isomer additional signals are seen between 320 and 340 K at 986 and 3013 cm^{-1} corresponding to the $\delta_{oop}(=C-H)$ and $\nu(=C-H)$ modes, respectively, so dehydrogenation may occur at only one of the central carbons at that stage. In fact, the peaks observed for $\nu(C-F)$ and $\gamma(CH_2)$ at 1010 and 1427 cm^{-1} , respectively, indicate the tilted nature of at least one of the terminal monofluoromethyl groups, and suggest an asymmetry in the moiety. Regardless, the spectra above 350 K for both isomers are similar, and show only a strong feature at 1370 cm^{-1} for the $\omega(CH_2)$ mode and weaker peaks at ~ 1030 , 1050 – 1100 (broad), and $\sim 2910\text{ cm}^{-1}$ for the $\rho(CH_2)$, $\nu(C-C)$, and $\nu(CH_2)$ vibrations, respectively. All evidence for the existence of internal C–H bonds is gone at this point, so the new species formed on the surface is likely to resemble adsorbed 1,4-difluoro-2-butyne. The same chemistry

has already been reported for normal 2-butenes on Pt(111).^{14,37} It should also be said that our data are inconsistent with the $M-CH=CH-CH=CH-M$ intermediate identified on other surfaces.³⁸

Complementary information on the high-temperature chemistry of the difluorobutenes was obtained by TPD. Representative traces for the evolution of hydrogen and hydrogen fluoride as a function of temperature are reported in Figure 6 for the *trans* isomer; the data for the *cis* case look quite similar (not shown). The top two traces in Figure 6 correspond to H_2 and HF desorbing from a clean Pt(111) surface saturated with *trans*-1,4-difluoro-2-butene. The hydrogen trace displays three main features, peaking at approximately 310, 385, and 640 K. The first peak is reasonably sharp, and corresponds to an average yield of two out of the six hydrogen atoms in the molecule. The temperature range involved and this stoichiometry are consistent with the formation of the acetylenic surface species mentioned in the previous paragraph.

A second H_2 desorption peak starts at around 340 K, and peaks at about 385 K. This is accompanied by a large HF desorption feature, which peaks at a slightly higher temperature, about 400 K. The exact overall stoichiometry of the surface moieties that form after this desorption is difficult to assess because that requires knowledge not only of the relative mass spectrometer sensitivities for H_2 vs HF but also of the amount of hydrogen consumed in the hydrogenation of the difluorobutene to difluorobutane. Nevertheless, it is estimated that an average of about two more hydrogens are extracted from the molecule in this temperature regime. It could also be inferred that all the fluorine is removed from the surface species as well, since no other fluorine-containing molecules were detected in the TPD experiments. This would leave an adsorbed moiety with C_4H_2 stoichiometry behind after heating to approximately 500 K, a species that then dehydrogenates in a broad temperature range peaking at about 640 K. A similar high-temperature intermediate has been reported to form on Pt(111) from butene, butadiene, and butyne.³⁹

Hydrogen fluoride desorption traces are also reported in Figure 6 for cases where the *trans*-1,4-difluoro-2-butene was dosed on hydrogen- (HF, middle trace) or deuterium (HF and DF, bottom two traces)-presaturated Pt(111). In both cases the yields are lower than on the clean surface, a result consistent with the lesser extent to which the molecule decomposes. In addition, hydrogen fluoride desorption occurs at lower temperatures, in two regimes peaking at about 260 and 350 K. It is interesting to note that some decomposition starts at about 200 K, simultaneously with the hydrogenation to the alkane. Nevertheless, the bulk of the decomposition, responsible for more than 75% the HF produced, occurs above 300 K.

Finally, the experiments with coadsorbed deuterium provide some additional information on both the extent of the H–D exchange that occurs at lower temperatures and the mechanism of decomposition. For one, it is noted that the DF yield amounts to about 30% of the total hydrogen fluoride detected, a result that indicates substantial isotopic substitution (an average of at least one H–D exchange per molecule). The extent of the exchange was less obvious in the traces for alkane desorption, but that may be easily explained by the relatively high temperatures required for the former reaction. On the other hand, a significant fraction of the DF formed desorbs below 300 K: that peak represents about half of all the DF produced, compared with only about 15% of the HF yield. Given that H–D exchange is known to occur preferentially at the inner carbon positions,^{4,9,10,40} this suggests that the low-temperature hydrogen

fluoride desorption is mainly the product of a recombination of fluorine atoms from the terminal monofluoromethyl groups with the hydrogen (deuterium) atom in the adjacent central carbon. A less selective reaction is operative above 300 K.

4. Conclusions

In this report we summarize the results obtained from RAIRS and TPD studies on the thermal chemistry of *cis*- and *trans*-1,4-difluoro-2-butenes on Pt(111) single-crystal surfaces. The motivation behind this work was to directly test the selectivity of *cis*–*trans* isomerization reactions, prompted by the indication from previous research with normal 2-butenes that Pt(111) surfaces may promote the thermodynamically unfavorable conversion of *trans* olefins to their *cis* counterparts. The opposite *cis*-to-*trans* conversion was seen here, but this apparent contradiction was explained by the role played by coadsorbed hydrogen, which appears to reverse the stability of the *cis* vs *trans* adsorbates on the surface.

Several additional differences were also identified when contrasting with the surface chemistry of regular 2-butenes, induced by the electronegative nature of the fluorine substituents. First, the adsorption of the difluoro-substituted olefins is significantly weaker than that of the regular 2-butenes. This leads to an easy collective change in low-temperature adsorption mode, from di- σ to π bonding, as the surface coverage is increased (in contrast with the build-up of a second π state on top of the preexisting di- σ layer seen with most other olefins). The fluorine substitutions also lead to a reduction in the extent of early H–D exchange when in the presence of coadsorbed deuterium, minimizing the amount of exchanged olefins detectable in TPD experiments. On the other hand, hydrogenation reactions are enhanced, and significant yields are seen for the resulting alkanes. Isotope scrambling does take place at higher temperatures, and is manifested by the production of H–D exchanged alkanes and by the considerable amount of DF also detected in TPD experiments. Dehydrogenation of the alkenes that remain on the surface leads to the formation of an acetylenic intermediate, as with the normal 2-butenes, but hydrogen fluoride elimination is also seen, initially via recombination of fluorine atoms with vinyl hydrogens.

Acknowledgment. Funding for this project was provided by the U.S. National Science Foundation under contracts NSF-CHE-0742414 and NSF-CHE-0316515.

References and Notes

- (1) Zaera, F. *Chem. Rev.* **1995**, 95, 2651.
- (2) Zaera, F. *Langmuir* **1996**, 12, 88.
- (3) Zaera, F.; Chrysostomou, D. *Surf. Sci.* **2000**, 457, 71.
- (4) Ma, Z.; Zaera, F. *Surf. Sci. Rep.* **2006**, 61, 229.
- (5) Salmerón, M.; Somorjai, G. A. *J. Phys. Chem.* **1982**, 86, 341.
- (6) Bertolini, J. C.; Massardier, J. Hydrocarbons on metals. In *The Chemical Physics of Solid Surfaces and Heterogeneous Catalysis*; King, D. A., Woodruff, D. P., Eds.; Elsevier: Amsterdam, The Netherlands, 1984; Vol. 3B (Chemisorption Systems), pp 107.
- (7) Bent, B. E. *Chem. Rev.* **1996**, 96, 1361.
- (8) Bond, G. C. *Metal-Catalysed Reactions of Hydrocarbons*; Springer: New York, 2005.
- (9) Morales, R.; Zaera, F. *J. Phys. Chem. B* **2006**, 110, 9650.
- (10) Morales, R.; Zaera, F. *J. Phys. Chem. C* **2007**, 111, 18367.
- (11) Lee, I.; Zaera, F. *J. Am. Chem. Soc.* **2005**, 127, 12174.
- (12) Lee, I.; Zaera, F. *J. Phys. Chem. B* **2005**, 109, 2745.
- (13) Zaera, F. *J. Mol. Catal. A* **2005**, 228, 21.
- (14) Lee, I.; Zaera, F. *J. Phys. Chem. C* **2007**, 111, 10062.
- (15) Polanyi, M.; Horiuti, J. *Trans. Faraday Soc.* **1934**, 30, 1164.
- (16) Zaera, F. *J. Phys. Chem. B* **2002**, 106, 4043.
- (17) Zaera, F. *Catal. Lett.* **2003**, 91, 1.
- (18) Delbecq, F.; Zaera, F. Submitted for publication.
- (19) Gellman, A. *J. Acc. Chem. Res.* **2000**, 33, 19.

- (20) Zhao, Q.; Zaera, F. *J. Am. Chem. Soc.* **2003**, *125*, 10776.
(21) Ye, P.; Gellman, A. J. *J. Phys. Chem. B* **2006**, *110*, 9660.
(22) Hoffmann, H.; Griffiths, P. R.; Zaera, F. *Surf. Sci.* **1992**, *262*, 141.
(23) Janssens, T. V. W.; Zaera, F. *J. Catal.* **2002**, *208*, 345.
(24) Zaera, F.; Chrysostomou, D. *Surf. Sci.* **2000**, *457*, 89.
(25) Pattison, F. L. M.; Norman, J. J. *J. Am. Chem. Soc.* **1957**, *79*, 2311.
(26) Durig, J. R.; Costner, T. G.; Goodson, B. J. *Raman Spectrosc.* **1993**, *24*, 709.
(27) Durig, D. T.; Herrebout, W. A.; Qiu, H. Z.; Zhen, M.; Durig, J. R. *Struct. Chem.* **1996**, *7*, 1.
(28) Guirgis, G. A.; Zhen, H.; Robb, J. B., II; Durig, J. R. *Vib. Spectrosc.* **2000**, *23*, 137–150.
(29) Sheppard, N.; de la Cruz, C. *Adv. Catal.* **1996**, *41*, 1.
(30) Greenler, R. G. *J. Chem. Phys.* **1966**, *44*, 310.
(31) Zaera, F. *Int. Rev. Phys. Chem.* **2002**, *21*, 433.
(32) Wilson, J.; Guo, H.; Morales, R.; Podgornov, E.; Lee, I.; Zaera, F. *Phys. Chem. Chem. Phys.* **2007**, *9*, 3830.
(33) Öfner, H.; Zaera, F. *J. Phys. Chem.* **1997**, *101*, 396.
(34) Somorjai, G. A.; Rupprechter, G. *J. Phys. Chem. B* **1999**, *103*, 1623.
(35) Zaera, F. *Acc. Chem. Res.* **2002**, *35*, 129.
(36) Doyle, A. M.; Shaikhutdinov, S. K.; Freund, H. J. *J. Catal.* **2004**, *223*, 444.
(37) Avery, N. R.; Sheppard, N. *Surf. Sci.* **1986**, *169*, L367.
(38) Ormerod, R. M.; Lambert, R. M.; Hoffmann, H.; Zaera, F.; Yao, J. M.; Saldin, D. K.; Wang, L. P.; Bennett, D. W.; Tyspe, W. T. *Surf. Sci.* **1993**, *295*, 277.
(39) Avery, N. R.; Sheppard, N. *Proc. R. Soc. A* **1986**, *405*, 1.
(40) Jenks, C. J.; Bent, B. E.; Zaera, F. *J. Phys. Chem. B* **2000**, *104*, 3017.

JP804360Z